Publications of the Astronomical Society of the Pacific
105: 487–493, 1993 May

Periodic Low-Amplitude Variations in the Brightness of Proxima Centauri[1]

G. F. BENEDICT, E. NELAN, B. MCARTHUR, AND D. STORY

McDonald Observatory, University of Texas, Austin, Texas 78712
Electronic mail: fritz@dorrit.as.utexas.edu, nelan@scivax.stsci.edu, story@scivax.stsci.edu, mca@astro.as.utexas.edu

W. VAN ALTENA

Yale University, Department of Astronomy, P.O. Box 6666, New Haven, Connecticut 06511
Electronic mail: vanalten@yalastro.bitnet

YANG TING-GAO

Shaanxi Observatory, P.O. Box 18, Lintong, Shaanxi, People's Republic of China

W. H. JEFFERYS

Department of Astronomy, University of Texas, Austin, Texas 78712
Electronic mail: bill@bessel.as.utexas.edu

P. D. HEMENWAY, P. J. SHELUS, AND A. L. WHIPPLE

McDonald Observatory, University of Texas, Austin, Texas 78712
Electronic mail: paul@astro.as.utexas.edu, pjs@astro.as.utexas.edu, alw@astro.as.utexas.edu

O. G. FRANZ

Lowell Observatory, Mars Hill Road, 1400 West, Flagstaff, Arizona 86001
Electronic mail: ogf@lowell.edu

L. W. FREDRICK

Department of Astronomy, University of Virginia, Charlottesville, Virginia 22903
Electronic mail: lwf@virginia.bitnet

R. L. DUNCOMBE

Aerospace Engineering, University of Texas, Austin, Texas 78712
Electronic mail: aoug065@emx.utexas.edu

Received 1992 November 10; accepted 1993 February 9

ABSTRACT. Using data acquired with Fine Guidance Sensor #3 on board the *Hubble Space Telescope* we find that the brightness of Proxima Centauri varies with an amplitude of 0.01 mag and a period $P=41.6\pm0.6$ days. We interpret this variation as rotational modulation of star spots or bright regions in the photosphere of Proxima Cen. In a total of 89.36 min of monitoring over 212 days, we detected one major flare and three post-flare brightenings.

1. INTRODUCTION

A test field was observed with Fine Guidance Sensor (FGS) #3 aboard the *Hubble Space Telescope (HST).* Data were acquired to determine the precision and accuracy of FGS astrometry and to measure the character and size of possible secular scale changes. The astrometric results will be reported elsewhere. The test field was chosen to include an astrometrically interesting object, Proxima Centauri, the nearest star other than the Sun. We will continue to monitor Proxima Cen in an effort to determine an upper limit on unseen companions orbiting with periods between 20 and 200 days. This paper presents some new photometric results for Proxima Cen.

Each of the three FGS is a white light interferometer containing four photomultiplier tubes (PMT). A technical description of the instrument can be found in Bradley et al. (1991). Since an earlier test determined that FGS 3 can be used as a photometer (Benedict et al. 1992), it is possible to monitor the brightness of each observed object. The FGS aperture on the sky is a 5×5 arcsec square. Our initial motivation for analyzing the photometry came from the fact that Proxima Cen is a flare star (V645 Cen), though at the low end of activity relative to other flare stars (Kunkel 1973). We did catch a major flare. Of more interest, we have determined that Proxima Cen exhibits periodic low-amplitude brightness variations.

[1]Based on observations with the NASA/ESA *Hubble Space Telescope,* obtained at the Space Telescope Science Institute, which is operated by the Association of Universities for Research in Astronomy, Inc., under NASA Contract No. NAS5-26555.

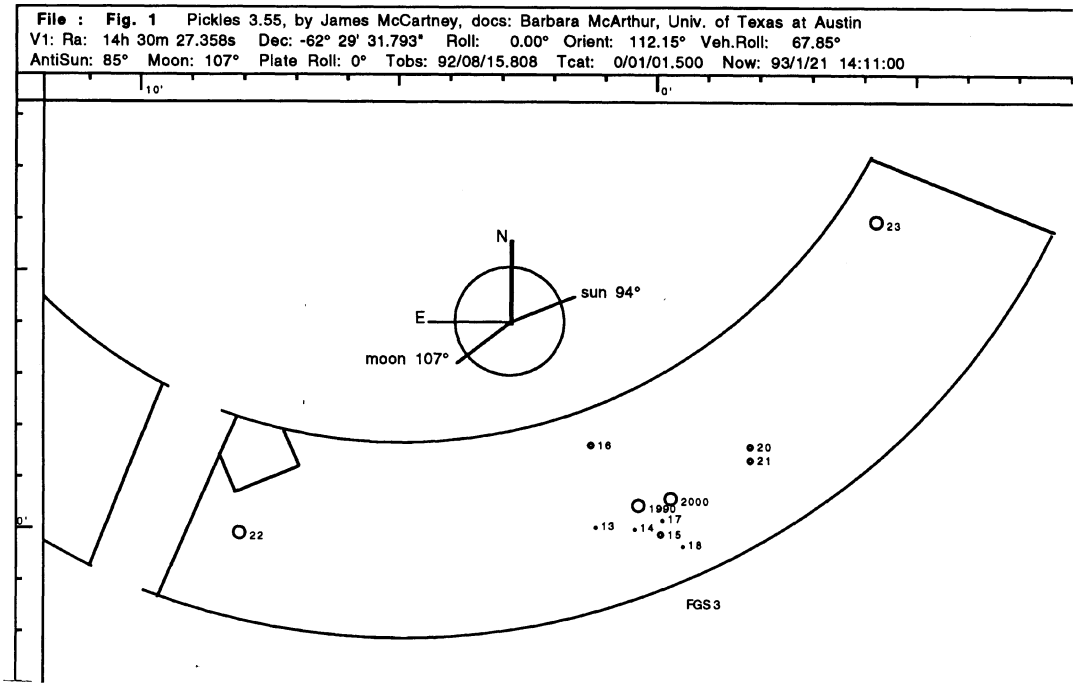

FIG. 1—Proxima Cen and reference stars within FGS #3. Positions for Proxima Cen are shown for epoch 1990.0 and 2000.0. Magnitudes for the reference stars are in Table 2. Orientation is nominal for 1992 August 15 (JD 2448849).

2. THE DATA

Our data consist of 33 sets of position measurements made with FGS 3 over 212 days. A position measurement is derived from a sequence of PMT readings reported back from *HST* at a 40 Hz rate. There are two PMT values per axis per 0.025 s. Most observations are between 60 and 90 s in duration. A final brightness measurement can consist of 4×2400 to 3600 individual readings.

Each observation set begins with a measurement of Proxima Cen, continues with a series of observations of nearby astrometry reference stars, and ends with a final measurement of Proxima Cen. Figure 1 presents a map of the monitored field which includes part of the *HST* focal plane arrangement. The stars are located within FGS 3. The position of Proxima is given for 1990 and 2000. The *HST* orientation is nominal for 1992 August 15. Nominal roll maximizes illumination of the *HST* solar arrays. The reference stars are observed in numerical order. Due to the changing roll orientation required to maintain maximum solar array illumination, not all reference stars are acquired during each observation set. In particular, the stars nearest the ends of FGS 3 were only observed ten times over 40 days.

The average time between the first and last measurements of Proxima Cen was 27 min. On five occasions we repeated the observing sequence on an immediately following orbit, affording a time delay of approximately 90 min. Thus, we sample the time domain unevenly with intervals ranging from 0.025 s, 27 min, through 90 min, several days, and up to ten days.

A log of the Proxima Cen observation and exposure times is presented in Table 1. All the day numbers used in this paper are a modified Julian Day (JD). Day=JD −2448000. The first Proxima Cen observation is always longer than the second within each observation set. This is

TABLE 1
Proxima Cen
Log of Observations

JD -2448000	V	V - <V>	Exp. T (sec)	JD -2448000	V	V - <V>	Exp. T (sec)
705.358	11.037	0.015	93.6	828.022	11.026	-0.002	92.4
705.371	11.033	0.011	66.5	828.039	11.031	0.003	79.4
714.325	11.037	0.016	92.6	830.968	11.037	0.009	92.3
714.338	11.029	0.007	66.5	830.987	11.036	0.008	64.5
724.308	11.025	0.004	92.4	831.029	11.038	0.010	92.3
724.321	11.025	0.003	66.5	831.049	11.025	-0.003	64.5
736.897	11.017	-0.004	93.5	845.831	11.031	0.003	92.4
736.910	11.014	-0.007	67.5	845.848	11.029	0.001	79.5
751.890	11.033	0.012	92.4	845.697	11.023	-0.005	92.4
751.905	11.030	0.009	66.5	845.716	11.025	-0.003	64.5
757.009	11.030	0.008	92.4	845.759	11.029	0.001	93.5
757.024	11.027	0.006	66.3	845.778	11.028	0.000	64.5
760.361	11.022	0.001	92.4	856.475	11.027	-0.001	92.4
760.374	11.024	0.003	66.5	856.492	11.028	0.000	79.4
770.208	11.017	-0.004	92.4	858.282	11.026	-0.002	92.4
770.221	11.019	-0.002	66.5	858.301	11.026	-0.002	64.5
784.202	11.034	0.013	92.4	858.344	11.028	0.000	92.4
784.216	11.030	0.008	66.6	858.363	11.024	-0.004	64.5
790.630	11.031	0.010	92.4	859.214	11.025	-0.003	92.4
790.643	11.028	0.007	67.4	859.233	11.021	-0.007	64.4
813.022	11.008	-0.013	91.9	859.276	11.026	-0.002	92.7
813.036	11.012	-0.009	62.4	859.295	11.023	-0.005	64.4
814.162	11.010	-0.012	92.4	867.321	11.028	0.000	92.4
814.181	11.008	-0.013	64.5	867.338	11.029	0.001	79.4
814.224	11.008	-0.014	92.4	876.726	11.036	0.008	92.4
814.243	11.007	-0.014	64.5	886.634	11.027	-0.001	92.3
819.921	11.012	-0.009	92.3	886.652	11.027	-0.001	79.4
819.938	11.014	-0.007	79.4	897.479	11.021	-0.007	92.4
823.871	11.009	-0.012	92.3	897.497	11.019	-0.009	79.5
823.890	11.012	-0.010	64.5	906.584	10.984	-0.044	92.6
823.933	11.021	0.000	92.4	906.601	11.022	-0.006	79.4
823.952	11.020	-0.001	64.5	917.084	11.059	0.031	92.4
				917.097	11.059	0.031	79.5

TABLE 2
Reference Stars in the Proxima Cen Field

Star ID	RA	DEC	V	B-V
Proxima	14h 29m 43.003s ± 0.008s	-62° 40' 46.1" ± 0.08"	11.02 ± 0.08	1.94 ± 0.08
13	14 29 55.664 0.004	-62 41 21.3 0.08	15.10 0.07	0.72 0.10
14	14 29 49.109 0.024	-62 41 21.6 0.17	15.76 0.06	0.87 0.17
15	14 29 44.491 0.006	-62 41 28.8 0.08	14.36 0.11	0.66 0.14
16	14 29 56.659 0.003	-62 39 44.5 0.07	14.58 0.09	0.52 0.12
17	14 29 44.281 0.006	-62 41 12.8 0.08	15.32 0.08	0.73 0.12
18	14 29 40.875 0.012	-62 41 41.5 0.15	15.14 0.05	1.53 0.07
20	14 29 29.567 0.007	-62 39 45.6 0.10	14.30 0.11	1.05 0.15
21	14 29 29.423 0.006	-62 40 2.3 0.07	14.43 0.09	0.69 0.13
22	14 30 55.728 0.033	-62 41 26.3 0.50	11.83 0.6	- -
23	14 29 8.998 0.033	-62 35 23.9 0.50	11.19 0.6	- -

Positions are J2000.0
Epoch of Proxima is 2000.0

an idiosyncrasy of the *HST* scheduling system. Our request was always for equal exposure times of 60 s. The actual exposure times were always longer than requested. The *HST* commanding system requires that sufficient time be allocated for a worst-case acquisition (Benedict et al. 1992). Usually the target is acquired early, resulting in increased time on target.

2.1 Photometric Reference Stars

Positions, magnitude, and color information for the stars in Fig. 1 are presented in Table 2. The astrometry and photometry are from a photographic study carried out by Yang and van Altena at Yale University. Note that the last two stars in Table 2 have less accurate positions and magnitudes and no colors. Information for these stars is obtained from the *STScI Guide Star Catalog* and is used only for relative, not absolute, photometric calibration.

2.2 Internal Errors

Telemetry from an FGS consists of readings from each of the four PMTs at a 40 Hz rate. Table 3 contains the average counts per 25 ms recorded on day 814.17 (Table 1) for the reference stars. We next list the total count per PMT for an average 90 s observation. The photometric noise is Poisson (Benedict et al. 1992). The 1-σ errors for the sums of the four PMTs are given in the last column of Table 3. For Proxima Cen ($V=11.02$) and a 60 s integration we expect 0.0014 mag 1-σ precision, and 0.001 mag for a 90 s integration.

TABLE 3
Expected Internal Photometric Errors

Star ID	V	per PMT (counts/0.025s)	per PMT total (count/90s)	error/90s observation (magnitude)
13	15.10	23	82800	0.008
14	15.76	13	46800	0.010
15	14.36	44	158400	0.005
16	14.58	35	126000	0.006
17	15.32	17	61200	0.009
18	15.14	23	82800	0.008
20	14.30	44	158400	0.005
21	14.43	38	136800	0.006
22	11.83	743	2674800	0.001
23	11.19	996	3585600	0.001

2.3 Calibration

We can provide precise but not particularly accurate V magnitudes for Proxima Cen. Our observations are through a broadband filter, F583W, having a full width half maximum of 234 nm centered at 583 nm. This is roughly a V bandpass. We have no color information in the instrumental system. Comparing the instrumental fluxes (averages for the first 14 observation sets) for the stars with measured $B-V$ in Table 1, we find no statistically significant dependence on color. Hence, we simply derive a zero point from the Table 1 standard magnitudes and apply it to the Proxima Cen measures.

2.4 Proxima Centauri

We follow standard techniques used in variable star photometry. One compares the signal from the star of interest to (often) a single reference star, presumed nonvariable (cf. Dorren and Guinan 1982). If the target star and reference star are observed in close enough temporal proximity, the brightnesses of the target and reference star are similarly modified by changes in telescope-photometer throughput and atmospheric transparency. Any differences between the flux from the two stars is attributed to the target star. In essence one "flat fields" the target star using the reference star.

Why is flat fielding necessary for these *HST* data? Observing from space, we have no transparency variations. Our sky level is very small (primarily galactic background light from unresolved stars) and constant. Unfortunately, *HST* is not a static, unchanging device. There is a slow defocus due to changes in the metering truss, the structure which holds the primary and secondary mirrors in mutual alignment. This primary–secondary separation change occurs as a result of carbon–graphite epoxy outgassing. Since the FGS field of view samples the focal plane at the edge, an average 12 arcmin from the center, the FGS works with large images. By changing the focus, we expect that the point spread function will vary, possibly changing the flux through our 5 arcsec aperture. This effect would be particularly apparent just before and after the infrequent commanded secondary mirror moves, when *HST* is refocused to correct for the slow defocus.

As in surface photometry, the less noise in the flat field, the better the photometry. Unfortunately, for the 212-day duration of this study the only stars included with Proxima Cen in every observation set were the faintest, stars 13 through 18 (Fig. 1). To decrease the noise, we have pieced together a flat field using the brightest sources available over various time spans. We first sum the fluxes from stars 15 and 16, the brightest stars available for all observation sets. The variation with time of this sum (normalized to the average for the interval between and including days 705 to 840) is plotted in Fig. 2. For a lesser duration we can sum stars 15, 16, 20, and 21, normalized as above. It is obvious that utilizing either of these sets of fainter stars as a flat field would introduce significant noise into the Proxima Cen data.

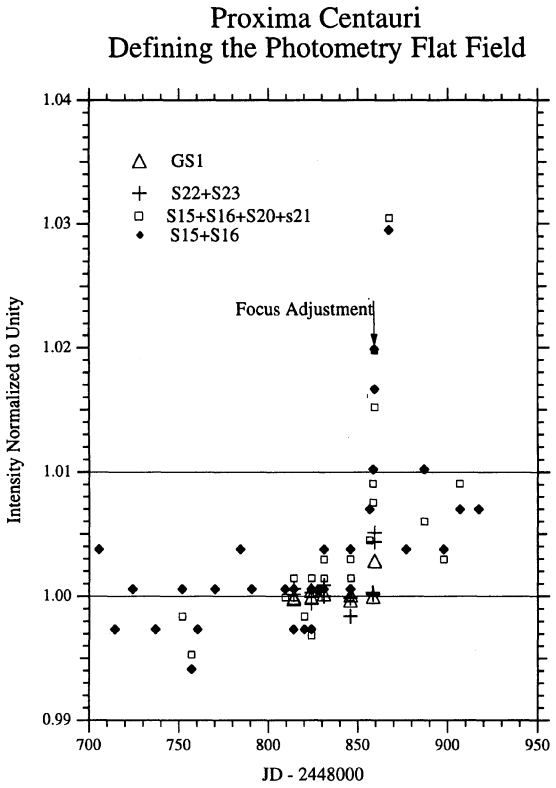

FIG. 2—Variations in reference or guide star signal expressed as ratios of signal over average signal between days 700 and 850. The secondary mirror was moved 14 μm on day 859 to refocus *HST*. The strongest signals have the smallest dispersion about unity and the smallest variation due to focus. From this distribution we abstract a flat response before focus and a 0.5% increase in signal after focus.

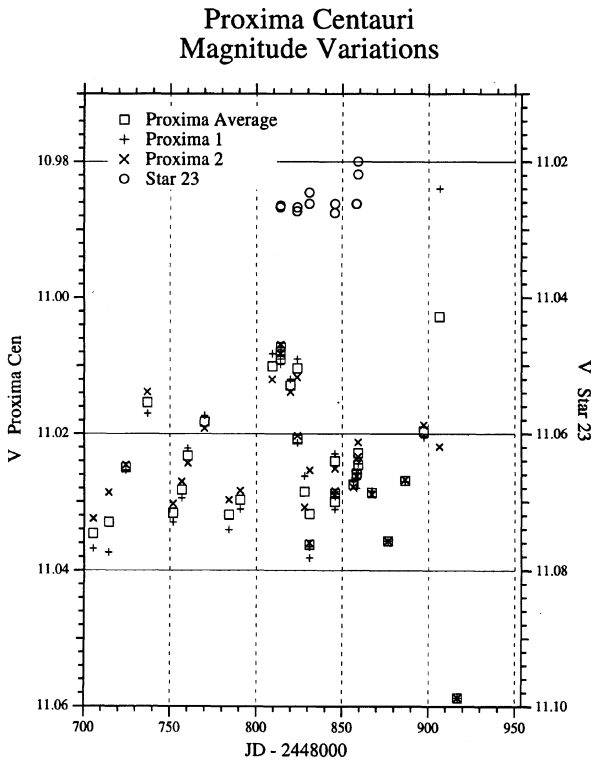

FIG. 3—Variations in the brightness of Proxima Cen expressed as magnitudes. The three symbols associated with each measurement are the first and second Proxima Cen observations and the mean of these. Values have been flat fielded. In support of the reality of these variations we also plot the brightness of reference star 23. The star 23 values have not been flat fielded to show the response to the refocus at day 859.

The much brighter stars 22 and 23 (Table 2) are observed for even a smaller interval, but do span a critical *HST* refocus event. These fluxes are normalized to the average between days 815 and 857. Finally, we plot the normalized flux from the guide star used in FGS #1, during this same interval, similarly normalized. The average flux through the 2/3 aperture used for all *HST* guiding (Benedict et al. 1992) was 779 counts per 0.025 s per PMT.

The arrow in Fig. 2 at day 858.8 indicates a refocus move of the secondary, amounting to 14 μm change in the primary–secondary separation. The variations in Fig. 2 are consistent with no flat-field variations prior to day 859, given the photometric errors shown in Table 3. The brighter stars indicate no flat-field variations prior to day 859 and a 0.5% increase after. Based on Fig. 2 and the internal noise (Table 3) we define the following simple flat field; no flat-field variations, except the 0.5% step response at and after day 859. We note that for sums with greater flux, the variations are smaller. We have no explanation for the large post-refocus variation in the fainter star sums, and point out that the latest data points have returned to near the 0.5% level. The return to a level consistent with the bright stars would seem to rule out a focus change having a greater effect in the center of the pickle than at the edges.

In Fig. 3 we present the calibrated Proxima Cen data. Each individual measurement (two per observation set) is plotted along with the per observation set average magnitude. Over the 212 days of this study for Proxima $\langle V \rangle = 11.025$. Compare with $V = 11.11$ (Cousins 1980) and $V = 11.22$ (Walker 1981). Cousins notes some disagreement among his measures taken 1977–79. Note that BY Draconis, the prototype, exhibits variations of 0.5 mag (Petterson et al. 1992) over many years. A list of the calibrated magnitudes and differences from the mean magnitude are presented in Table 1.

We believe that the Proxima Cen variations shown in Fig. 3 are real. There is no flat-field structure in Fig. 2 which agrees in amplitude and phase with the Proxima Cen variations. Finally we plot (Fig. 3) the calibrated magnitude of star 23. The observations in close temporal proximity (days 814, 823, 830, 845, and 858) are separated by about 90 min. We observe star 23 only once per orbit. Prior to day 859, the rms scatter about the mean is 0.0007 mag over 44 days. The obvious discontinuity on day 859 is due to a 14 μm secondary mirror *HST* refocus move. This motion results in a 0.005 mag change.

3. DISCUSSION AND CONCLUSIONS

The light curve presented in Fig. 3 seems to indicate periodic behavior. But, Proxima Cen is a known flare star.

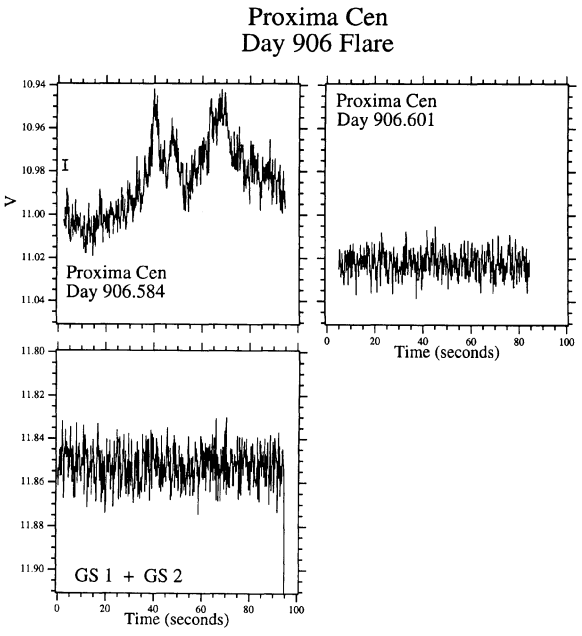

FIG. 4—One second time resolution photometry for (a) Proxima Cen, flaring, (b) the sum of guide stars one and two, and (c) a Proxima Cen observation 25 min after the flare. (a) and (b) are simultaneous observations. 1-σ error bars are displayed in each panel.

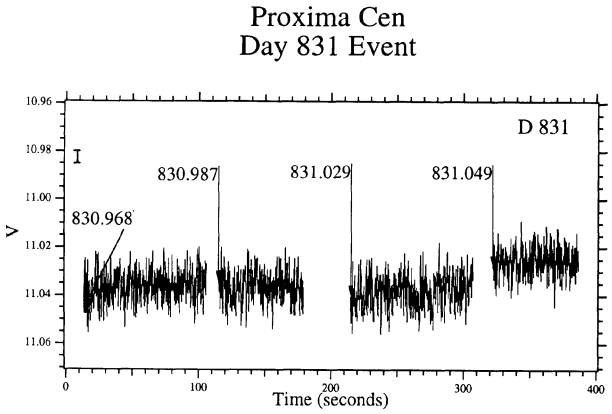

FIG. 5—One second time resolution photometry for Proxima Cen. The last time series shows Proxima Cen 0.011 magnitude brighter than the previous level, obtained 29 min earlier. A 1-σ error bar is displayed.

In this section we attempt to identify the flare-related structure in Fig. 3, remove it, and derive a period. Lastly we offer an interpretation of these data.

3.1 Flare Activity

Flares are short lived (usually less than 1 min) and are primarily ultraviolet phenomena. For typical flare colors ($B-V=-0.10$ and $U-B=-1.11$, Kunkel 1970b) a $\Delta U=-2.5$ event would have only a -0.1 mag effect in V for Proxima Cen. Our flare detection criterion is that the two Proxima Cen observations separated by an average 27 min must have a greater than 3-σ difference, 0.006 mag at $V=11.02$. The events which meet this criterion are easily discernible in Fig. 3 at days 714.32, 831.02, and 906.08.

Figure 4 shows the time evolution of the day 906 flare. The data have been binned with 1-s resolution, providing a 1-σ photometric error of 0.0054. mag. The flare occurred during the first of the two Proxima Cen observations made that day. The second observation, 25 min later, is also plotted, showing that the star had returned to a quiescent level. The two bright peaks ($\Delta V=-0.055$) were likely caused by $\Delta U=-1.88$ flares. To demonstrate that this activity is not related to increased particle flux from the South Atlantic Anomaly, we also plot a relative magnitude derived from the sum of the fluxes for the guide stars in FGS #1 and FGS #2. This is a flat distribution.

On day 831 we see a brightening of $\Delta V=0.011$ between two observations separated by 29 min. Yet, when we plot (Fig. 5) the time evolution for each observation acquired, we find very little structure. The supposed flare event took place in the last set. Again, to eliminate any on-orbit environmental factors, we inspect the fluxes for stars 22 and 23, observed within several minutes of Proxima Cen. Figure 2 indicates a only a 0.1% difference. The day 714 event is similar, with no obvious flare signature.

Fitting straight lines to the day 714.325 and 831.049 time series (the latter shown in Fig. 5), we find very small but statistically significant negative gradients, indicating a slight Proxima dimming. Walker (1977) displays flares (his events 15 and 30) where the decline from maximum light is very slow. Our day 831 and 714 events might be far out on the tail of such a flare.

There is one other event on Fig. 3 which might be flare related. At day 823 we secured two sets of observations separated by 1.5 h. The set starting at day 823.871 is an average 0.012 mag brighter than the day 823.933 set. Referring once again to Fig. 2, we see the variations in the bright stars 22 and 23 are at or less than 0.1%, supporting the reality of the Proxima Cen changes. Again we see no explicit flare signature in the time-resolved data. Presumably this observation set also caught the tail end of a large flare.

Bright flares are relatively rare. For Proxima Cen Kunkel (1970a) observed only two $\Delta U=-2.5$ events in 23.6 h. Over the 212-day duration of the test, we observed Proxima Cen a total of 89.36 min. We see no 0.1 mag variations, consistent with this rarity. What of our obvious day 906 flare? Using the prediction algorithm of Kunkel (1973), the expectation is for one $\Delta U=-1.88$ event in 280 min. Assuming the flare lasts 30 s, Walker (1981) predicts one event of this energy every 302 min, based on a flare production rate analysis derived from 25 h of monitoring. Observing such a flare in 89 min is consistent with both predictions.

3.2 Periodic Photometric Variations

Having identified some of the variations in Fig. 3 with flare activity, we remove these events and apply two techniques to the remaining Proxima Cen data to determine a period. The two techniques used, sin curve fitting, and pe-

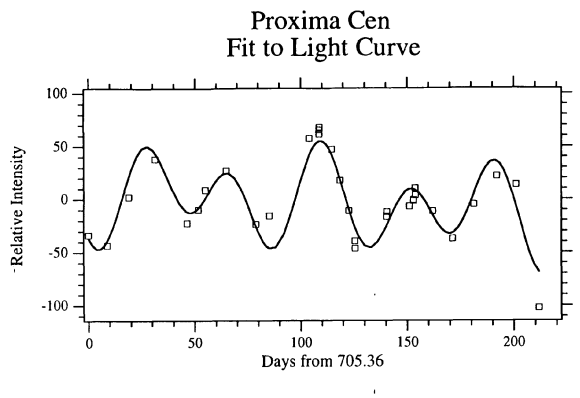

FIG. 6—Differential light curve for Proxima Cen. Differences are average counts during the observation for a sum of the four PMT. A difference of 40 counts is about 1%. The symbols are about the error bar size. Also shown is a fit to a function consisting of two sin waves and a sloping linear background.

riodogram analysis, are equivalent, but yield slightly different results. In all cases we work with the Proxima Cen intensity variations around the mean value, a differential intensity light curve. We first form the PMT sums per 0.025 s, averaged over the observation time given in Table 1. The actual data values (Fig. 6) are the difference between the 212-day average and the value for each observation.

Press and Teukolsky (1988) present an algorithm for searching for weak periodic signals in unevenly spaced data. Their algorithm also estimates the likelihood of the reality of any peak found in the resulting power spectrum. In other words we obtain the significance of the peak against the hypothesis of random noise. We first apply this tool to the summed intensities of reference stars 15 and 16, excluding data after day 858 [Fig. 7(a)]. The only periodic variation *HST* impresses on the photometry is a 20-day period caused by the least significant bit of the intensity sum bouncing back and forth.

Subjecting the differential intensity data of Fig. 6 to the same analysis [Fig. 7(b)] results in one peak at $P_1=41.3$ days with less than a 1% likelihood of being false positive. The longer, $P_2=68.4$ days, has a 50% chance of being false positive. This longer period is likely due to the periodogram program attempting to describe the changing peak brightness seen in Fig. 3 as a beat phenomenon.

Armed with these two major modes, we fit the light curve with a superposition of two sin waves on a sloping, straight-line background. The form of this 8 coefficient function is

$$I=I_0+I't+A_1\sin[(2\pi/P_1)+\phi_1]$$
$$+A_2\sin[(2\pi/P_2)+\phi_2].$$

The result of this curve fitting is shown in Fig. 6. The fit parameters are given in Table 4, along with derived uncertainties. The last column provides a significance parameter for each coefficient. We see that the linear trend has little significance. The periods are $P_1=41.84\pm0.52$ days with a

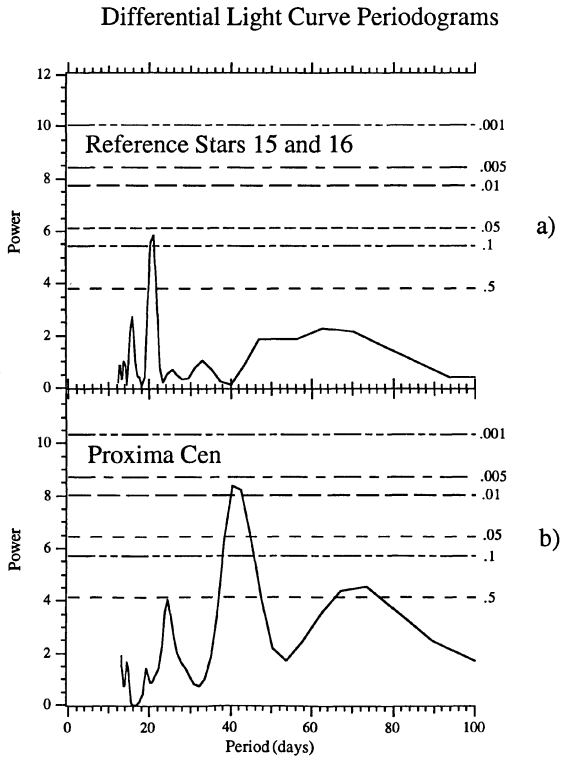

FIG. 7—Lomb-Scargle normalized periodograms. (a) The sum of reference stars 15 and 16, days 700 to 850. The 20-day period is easily identified as toggling in the least significant bit in the sum (see Fig. 2 for confirmation). (b) The Proxima Cen differential light curve shown in Fig. 6. The peak at $P=41$ days has less than a 1% chance of being due to noise. Comparing the two periodograms, we see that the *HST* system evidences no significant power at $P=41$ days.

1% amplitude and $P_2=70.29\pm2.42$ days with a 0.5% amplitude.

The average of these two techniques results in $P_1=41.5\pm0.5$ days and $P_2=69.3\pm2.4$ days, where the errors are taken from the curve fit.

3.3 Interpretation

Baliunas and Vaughan (1985) review similar low-amplitude brightness variations for BY Draconis stars and note that the phenomena usually occur in binary systems. Interaction between the components causes magnetic dis-

TABLE 4
Light Curve Fit

coefficient			units	coeff/sigma
I_o	10.71	±5.72	counts	2
I'	-0.12	0.05	counts/day	2
A_1	36.03	3.75	counts	10
P_1	41.84	0.52	days	80
ϕ_1	-2.24	0.23	radians	10
A_2	21.55	3.37	counts	6
P_2	70.29	2.42	days	29
ϕ_2	-2.06	0.4	radians	5

turbances which manifest themselves as star spots or bright regions in the stellar atmospheres. Rotation then modulates the brightenings or darkenings. Dorren and Guinan (1982) find low-amplitude variations in single stars. Again, assuming that rotation modulates the signal from dark or bright areas on the stellar surface, they find rotation periods ranging from 11 to 54 days.

As the spots or bright regions change in size and intensity, the peaks in Fig. 3 and 6 vary in height. Note that most of the minima are about the same level. This argues for rotationally modulated regions which vary in brightness, rather than spots which change size (Pettersen et al. 1992). Another possible interpretation consists of a longer period of rotation ($\sim$80 days) with two distinct bright regions on Proxima. The alternation of peak brightness (Fig. 6) supports this interpretation. However, the periods are not a close multiple of two. Far more monitoring will be required to determine the reality and/or physical significance of the longer period. Should our continuing observation series support the longer period, it becomes far more likely that 2 relatively cooler spots are involved, a situation similar to that found for 12 Ophiuchi by Dorren and Guinan (1982). We will analyze future data for differential rotation of a pair of spots. Finally, in support of faster rotation, Doyle (1987) predicts a rotation period $P=51 \pm 12$ days from the chromospheric activity of Proxima Cen.

Several studies have determined an age for α Centauri (Demarque et al. 1986; Furenlid and Meylan 1990) of 4–4.5 Gy. Flannery and Ayres (1978) obtain 6 Gy. Should the rotational interpretation of the brightness variations survive additional data, the age and rotation rate of Proxima Cen should provide an important constraint for magnetic braking theories (e.g., Soderblom 1985), assuming Proxima Cen to be coeval with α Cen.

3.4 Conclusions

The brightness of Proxima Cen varies periodically with an amplitude of 0.01 mag. We interpret the 41.5-day variation as rotational modulation of a star spot or bright region in the photosphere of Proxima Cen. In a total of 89 min of monitoring, we have detected one obvious flare and three other post-flare brightenings. Our astrometric and photometric monitoring of Proxima Cen with *HST* will resume in late 1992 December and conclude in 1993 May.

The senior author thanks David S. Evans, B. Bopp, and S. Hawley for providing a crash course in the star spot business. This note benefited from careful readings by E. Robinson (who first suggested the 80-day period interpretation), W. Cochran, and an anonymous referee. We acknowledge essential support from NASA Contract No. NAG5-1603.

REFERENCES

Baliunas, S. L., and Vaughan, A. H. 1985, ARAA, 23, 379
Bradley, A., Abramowicz-Reed, L., Story, D., Benedict, G., and Jefferys, W. 1991, PASP, 103, 317
Benedict, G. F., Nelan, E., Story, D., McArthur, B., Whipple, A. L., Jefferys, W. H., van Altena, Wm. F., Hemenway, P. D., Shelus, P. J., McCartney, J. E., Franz, O. G., Fredrick, L. W., Bradley, A., and Duncombe, R. L., 1992, PASP, 104, 958
Cousins, A. W. J. 1980, SAAO Circ., 1, 166
Demarque, P., Guenther, D. B., and van Altena, Wm. F. 1986, ApJ, 300, 773
Dorren, J. D., and Guinan, E. F. 1982, AJ, 87, 1546
Doyle, J. G. 1987, MNRAS, 224, 1p
Flannery, B. P., and Ayres, T. R. 1978, ApJ, 221, 175
Furenlid, I., and Meylan, T. 1990, ApJ, 350, 827
Kunkel, W. E. 1970a, Inf. Bull. Var. Stars, No. 462
Kunkel, W. E. 1970b, ApJ, 161, 503
Kunkel, W. E. 1973, ApJS, 25, 1
Pettersen, B. R., Hawley, S. L., and Fisher, G. H. 1992 Sol. Phys., 142, 197
Press, W. H., and Teukolsky, S. A. 1988, Comput. Phys., 2, 77
Soderblom, D. R. 1985, AJ, 90, 2103
Walker, A. R. 1977, M.N.A.S. So. Africa, 36, 97
Walker, A. R. 1981, MNRAS, 195, 1029